Contrib Mineral Petrol (1985) 89:394–409

Contributions to Mineralogy and Petrology

Geochemistry of phonolites and trachytes from the summit region of Mt. Kenya

R.C. Price[1], R.W. Johnson[2], C.M. Gray[1], and F.A. Frey[3]

[1] Geology Department, La Trobe University, Bundoora, Vic. 3083, Australia
[2] Bureau of Mineral Resources, GPO Box 378, Canberra 2601
[3] Department of Earth and Planetary Sciences, M.I.T., Cambridge, Massachusetts, 02139, USA

Abstract. Two suites of felsic eruptives and intrusives are represented in a set of samples from the summit region of the Plio-Pleistocene volcano, Mt. Kenya. Most of the samples are moderately or strongly undersaturated and have $^{87}Sr/^{86}Sr$ initial ratios in the range 0.70360–0.70368 (mean = 0.70362). Members of this phonolitic suite are phonolites, nepheline syenites or kenytes and as a group they show a wide variation in TiO_2, FeO, P_2O_5, Sr, Ba, Zr and Nb. The minor and trace element geochemistry reflect variation in the nature of the parental basaltic magmas from which the phonolitic rocks evolved and variation in the crystal fractionation process in individual cases. Crystal fractionation involving plagioclase, alkali feldspar, clinopyroxene, olivine and magnetite is the process by which most of the phonolitic rocks evolved and variation in the relative proportions of these phases in individual cases has led to a broad spectrum of trace and minor element behaviour.

The second suite of felsic samples is critically saturated and consists of trachytes showing either slight oversaturation or slight undersaturation with respect to SiO_2. This trachyte suite has lower initial $^{87}Sr/^{86}Sr$ ratios (mean = 0.70355) and is derived from transitional alkalic basalts by low pressure (crustal) crystal fractionation involving feldspar, clinopyroxene, magnetite and olivine.

The range in minor and trace element chemistry observed among the felsic rocks is a consequence of variation in the parental basalts which is related to mantle source variation and to the specific nature of the crystal fractionation process.

Introduction

Many phonolites and nepheline syenites have been interpreted as the end products of low pressure (crustal) fractional crystallization from basanitic or trachytic parental lavas (e.g. Coombs and Wilkinson 1969; Nash et al 1969; Ridley 1970; Lippard 1973; Price and Chappell 1975). Although some phonolitic rocks contain evidence of a high pressure (mantle) origin (e.g. Wright 1966, 1969; Price and Green 1972; Green et al. 1974) these can also be explained as melts derived from basanite by high pressure crystal fractionation processes (Irving and Price 1981). In some provinces the relative volumes of basaltic, phonolitic and intermediate lava types have been considered by some to be inconsistent with simple crystal fractionation models and it has been suggested (e.g. Bailey 1964; Bailey and Schairer 1966; Williams 1971; Woolley and Symes 1976) that phonolitic and trachytic melts could be derived by partial melting of basaltic material in the lower crust or upper mantle. Many petrologists find it difficult to choose between the partial melting and crystal fractionation models on the basis of the data available in specific cases (e.g. Gill 1972; Goles 1976).

This paper presents data for a suite of samples from the summit region of Mt. Kenya. The suite covers a range of phonolitic and trachytic compositions and provides an opportunity to examine the geochemical relationships between different alkalic compositions.

Geological setting. Mt. Kenya, which reaches a summit of 5,200 m is a central volcano located to the east of the East African Rift (Fig. 1).

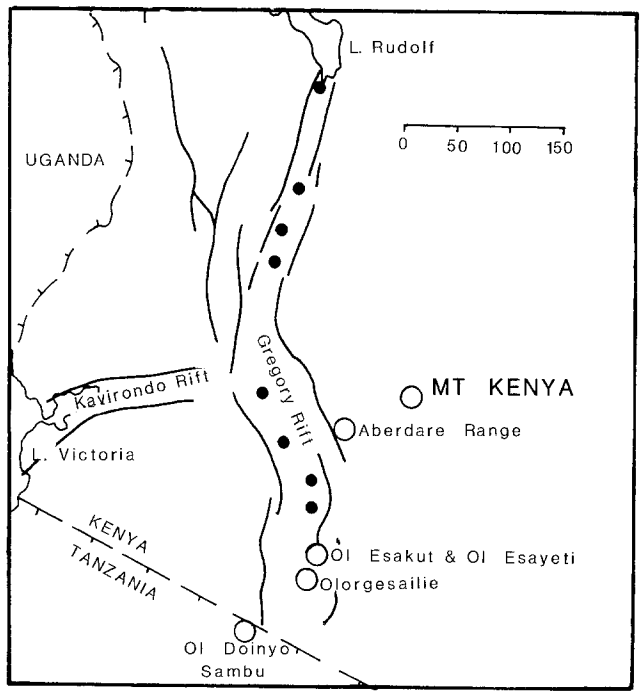

Fig. 1. Mt. Kenya, the Gregory Rift, and the East African Rift System. Pliocene central volcanoes (*circles*) and Quaternary central volcanoes (*filled circles*) are indicated. (Baker et al. 1971) Scale is in km

Offprint requests to: R.C. Price

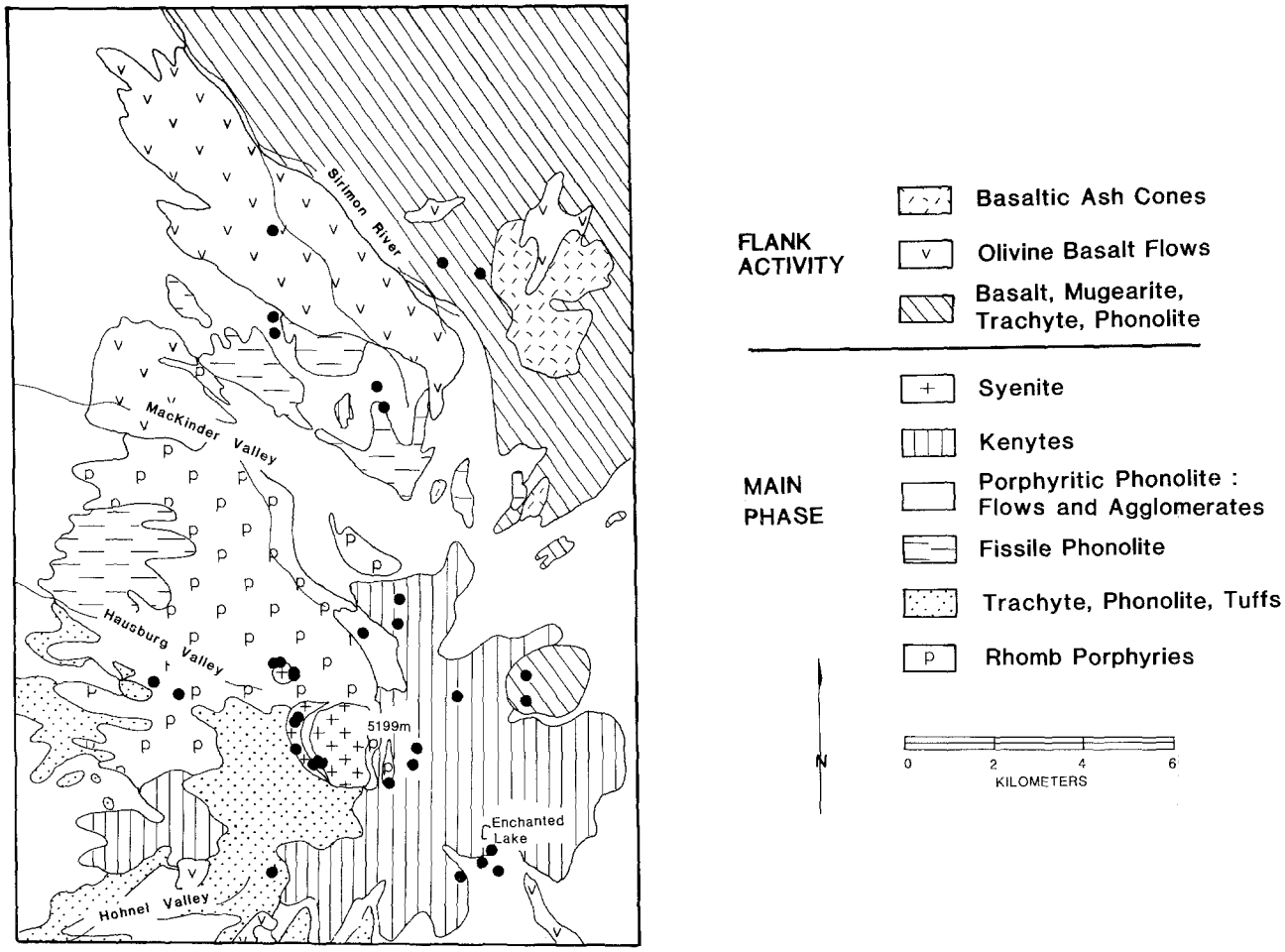

Fig. 2. Sketch map of upper portion of Mt. Kenya (from Baker 1967). Filled circles indicate samples used in this study

The main eruptive phase of the Mt. Kenya Volcanics is of Pliocene to Pleistocene age (Baker et al. 1971; Rock 1976) and overlies tuffs and basalts of Miocene-Pliocene age which rest on a Precambrian basement of gneisses and schists (Baker 1967). The main eruptive phase is composed of basalts, phonolites, kenytes and trachytes with the summit consisting of a complex intrusive plug of syenite and phonolite (Fig. 2). The most recent activity on Mt. Kenya occurred as satellite eruptions which built pyroclastic cones and extrusive domes of basalt and trachyte. These later eruptives, which were also extensively emplaced as dykes are believed to be of Pleistocene age (Baker 1967). Erosion of the summit by glaciers which are still active has extensively exposed the central core of the volcano making it possible to collect an excellent suite of fresh samples (Fig. 2).

Petrography

The locations of the samples which form the basis of this study are shown on Figure 2. The samples were collected by D.J. Jennings and R.W. Johnson in 1963. Most of the samples are phonolites or nepheline syenites although samples of basalts and trachytes have been included in the analyzed suite. Nomenclature follows Coombs and Wilkinson (1969) with some modifications (Price and Chappell 1975).

Phonolites. There is a spectrum of textural variation among the phonolitic rocks from strongly porphyritic to aphyric. Anorthoclase is the dominant phenocryst with nepheline, olivine, apatite, magnetite and, less commonly, pale green clinopyroxene occurring as phenocrysts. The groundmass of a typical phonolite is composed of alkali feldspar, nepheline, aegirine and aenigmatite. Fayalite, alkali amphibole and sodalite are present in some samples.

Baker (1967) distinguished three main types of phonolite that were important in the construction of a stratigraphic sequence for the summit region of the volcano. Porphyritic phonolites were classified by Baker as "rhomb porphyries" or "porphyritic phonolites". These are convenient field terms; the rhomb porphyries are highly distinctive rocks characterized by an abundance of large (1.5 cm) phenocrysts of rhombic feldspar. The porphyritic phonolites are distinct from the aphyric phonolites which were termed "fissile" by Baker (1967) because they have a well developed flow layering.

Kenytes. Kenytes are strongly porphyritic glassy rocks of phonolitic composition. On the summit of Mt. Kenya the kenytes are laterally equivalent to the porphyritic phonolites (Baker 1967). A typical kenyte is between 20 and 30% phenocrysts in a glassy flow-banded matrix. The phenocrysts, which range up to 2 cm in length are mainly anorthoclase with nepheline phenocrysts being less abundant. Olivine, apatite and magnetite are abundant as smaller phenocrysts (up to 2 mm). Clinopyroxene phenocrysts are rare and contain abundant inclusions of apatite, magnetite and glass. Aggregates of apatite and magnetite; clinopyroxene and olivine; and olivine, apatite and magnetite are common.

Syenites, nepheline-syenites, and microsyenites

The summit massif of Mt. Kenya is composed of an intrusive complex of syenite and phonolite. The syenites range in composi-

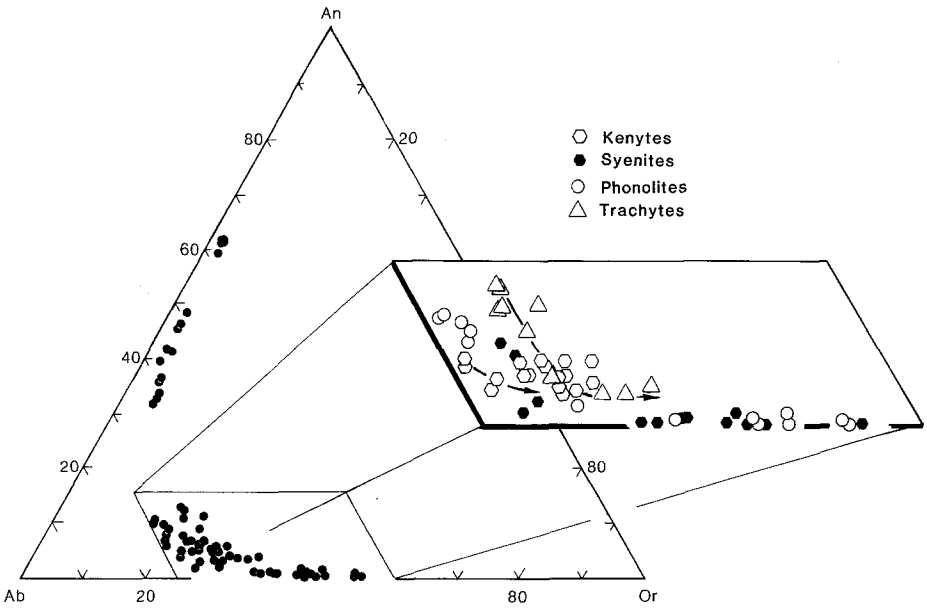

Fig. 3. Electron microprobe analyses of feldspars from the Mt. Kenya volcanics plotted in the system An-Ab-Or

tion from strongly to moderately undersaturated with respect to SiO_2 and different textural types are distinguished on the basis of abundance of phenocrysts and grain-size. The central intrusive complex is the subvolcanic equivalent of the phonolite-kenyte sequence.

A typical nepheline-syenite is medium- to coarse-grained (0.5 mm–1 cm) and mildly porphyritic. The phenocrysts are altered nepheline and perthitic alkali feldspar. Amphibole occurs as large (up to 0.5 cm) poikilitic crystals enclosing aegirine, aenigmatite and nepheline. In some cases the amphibole is zoned from pale brown cores to blue-brown rims. Pale clinopyroxene phenocrysts have aegirine rims.

Sodalite, apatite and magnetite are minor phases in most but can be important in some samples. One or two of the samples examined also contain olivine. In some samples pale orange biotite is common and riebeckite occurs in others. One microsyenite contains needles of woehlerite-lavenite ($\alpha = \beta$ = pale yellow; γ = very pale yellow). Many of the syenites and microsyenites are altered. In altered syenites biotite is abundant and replaces amphibole. Nepheline is altered to white mica. In some altered samples patches of carbonate are present and have a globular form which might indicate very late stage liquid immiscibility. The only zircon grains observed in the sample suite are in altered syenites with carbonate globules.

Late trachytes and phonolites

The main phonolitic eruptive phase of Mt. Kenya is post-dated by eruptive activity dominated by feldspathoidal trachyte, trachyte, and phonolite. Various textural types occur in this grouping of lavas and this is controlled by the abundance of phenocrysts. Many of these lavas are aphyric but some are strongly porphyritic (up to 40% phenocrysts). In typical feldspathoidal trachytes the matrix is flow-banded alkali feldspar, aegirine, apatite and magnetite with minor nepheline. Aenigmatite is present in some cases. Phenocrysts which range up to 1–2 mm in length are alkali feldspar and zoned plagioclase, fayalitic olivine, apatite and magnetite. Aggregates of magnetite in some trachytes may be pseudomorphing amphibole.

Quartz-normative peralkaline trachytes post-date the main eruptive event and were emplaced as small dykes and domes in the summit region (Baker 1967). A typical pantelleritic trachyte dyke rock is an even-grained and flow-textured rock with rare phenocrysts of pale-green clinopyroxene (up to 0.2 mm) and alkali feldspar (1 mm in length). The groundmass consists of alkali feldspar, aegirine, riebeckite, minor apatite and magnetite.

Mafic rocks. Of five basalt samples analyzed as part of this study four are olivine basalts and one is a basanite. Basaltic lavas associated with satellitic vents represent the most recent activity in the summit region of Mt. Kenya. Those on the north flank belong to the Nyambeni fissure phase (Baker 1967). An analyzed basanite is a mildly porphyritic rock consisting of plagioclase (An_{61}), augite, magnetite and apatite with phenocrysts of augite, olivine (Fo_{81}) and magnetite. The augite phenocrysts range up to 5 mm in maximum dimension and are zoned with clear cores and pink, seive-textured titaniferous rims. Lherzolite nodules up to 5 cm in diameter occur in the rock. Olivine basalts range compositionally from basalts in the strict sense through to mugearite. A typical olivine hawaiite contains phenocrysts (up to 1 mm) of plagioclase (An_{50-45}), olivine (Fo_{59}) and apatite in a groundmass of olivine (Fo_{55}), plagioclase (An_{42}), augite, apatite and magnetite.

Mineral chemistry

Feldspars. Variation in feldspar chemistry within the Mt. Kenya Suite is summarized in Fig. 3. Among the phonolites and kenytes alkali feldspar phenocrysts are zoned from sodium-rich cores to potassium-rich rims. The feldspar chemistry within the syenitic rocks is complicated by subsolidus unmixing but overall the trends observed in the eruptives are reflected in the intrusives. No single liquidus path is outlined and for most of the phonolitic rocks a single line of descent is not indicated by the feldspar chemistry.

Plagioclase phenocrysts are not common in the feldspathoidal trachytes but where they occur are strongly zoned and show extensive resorption. One example is zoned from An_{39} in the core to An_{31} on the rim.

Pyroxenes. Representative pyroxene analyses are presented in Table 1. Pyroxene phenocrysts in kenytes, nepheline syenites and phonolites are normal augites. The pyroxenes of the syenites are zoned to aegirine rims (Fig. 4); a trend which is reflected in the groundmass pyroxenes of the eruptives. Groundmass pyroxenes in the syenites and in some of the phonolites are higher in Ti and lower in Mg than the phenocrysts (Fig. 5). Al is higher in the pyroxenes of the kenytes than in the other phonolitic rocks. The pyroxene trends observed in the basaltic rocks are distinct from those

Table 1. Representative pyroxene analyses

	1	2	3	4	5	6	7	8	9	10	11	12	13	14
Sample[a] no:	52	22	4C	4R	11C	11G	46C	46G	54	20	38N	38C	38R	38G
SiO_2	50.92	51.22	53.51	53.07	52.02	51.67	51.83	47.86	51.01	49.70	47.74	48.46	46.80	47.22
TiO_2	0.23	1.01	1.01	1.42	0.45	2.15	0.49	1.79	0.70	0.63	1.45	1.67	3.03	2.51
Al_2O_3	1.59	2.10	0.73	0.64	0.93	1.14	1.38	4.19	1.73	1.66	7.40	7.76	5.70	5.28
FeO[b]	14.83	9.29	9.40	17.26	11.15	20.07	11.03	11.62	11.19	20.05	6.08	6.44	8.28	7.87
MnO	0.96	0.59	0.61	0.57	0.67	0.56	0.17	0.64	0.62	0.70	0.19	0.14	0.12	0.19
MgO	8.51	12.64	12.11	5.89	11.43	3.42	11.94	9.94	11.10	7.44	12.96	13.02	12.43	13.07
CaO	21.09	20.49	19.23	9.39	21.01	9.41	22.30	21.43	21.95	18.94	21.31	21.39	22.87	22.98
Na_2O	1.60	1.60	3.07	8.38	1.66	8.29	0.71	1.40	0.83	0.83	0.97	0.96	0.47	0.49
K_2O	0.10	0.01	0.03	0.02	0.01	0.07	0.02	0.12	0.05	–	–	–	–	0.01
Cr_2O_3	–	0.07	–	–	0.03	0.05			0.07		0.26	0.44	–	–
NiO	–	–	0.13	0.02	0.10	0.06			0.09		0.05	0.06	0.03	0.13
BaO	–	–	–	0.25	0.06	0.07			0.04		0.02	–		
Total	99.83	99.02	99.83	96.91	99.52	96.96	99.87	98.99	99.38	99.95	98.43	100.34	99.73	99.75
	Structural formulae on basis of 6 oxygens													
Si	1.970	1.920	2.007	2.103	1.981	2.077	1.955	1.849	1.948	1.940	1.797	1.790	1.768	1.782
Al^{IV}	0.030	0.080	–	–	0.019	–	0.045	0.151	0.052	0.060	0.203	0.210	0.232	0.218
Al^{VI}	0.043	0.013	0.032	0.030	0.023	0.054	0.016	0.040	0.026	0.016	0.125	0.128	0.022	0.017
Ti	0.007	0.028	0.029	0.042	0.013	0.065	0.014	0.052	0.020	0.019	0.041	0.046	0.086	0.071
Cr		0.002		–	0.001	0.001			0.002		0.008	0.013	–	–
Fe	0.480	0.291	0.295	0.572	0.355	0.675	0.348	0.375	0.357	0.655	0.191	0.191	0.262	0.248
Mn	0.032	0.019	0.019	0.019	0.022	0.019	0.023	0.021	0.020	0.023	0.006	0.004	0.004	0.006
Mg	0.491	0.707	0.677	0.348	0.649	0.205	0.671	0.572	0.632	0.433	0.727	0.717	0.700	0.735
Ni			0.004	–	0.003	0.002			0.003		0.002	0.002	0.001	0.004
Ca	0.874	0.823	0.773	0.399	0.857	0.405	0.901	0.887	0.898	0.792	0.859	0.846	0.926	0.929
Na	0.120	0.116	0.223	0.644	0.122	0.646	0.052	0.105	0.061	0.063	0.071	0.068	0.035	0.036
K	0.005	0.001	0.002	0.001	0.001	0.004	0.001	0.006	0.002	–	–	–	–	0.001
Ba				0.004	0.001	0.001			0.001		–	–		

[a] Refer to Tables 6 and 7 for rock types Subscripts denote the following: C = phenocryst core, R = phenocryst rim, G = groundmass, N = pyroxene in lherzolite nodule contained in basanite 38

[b] Total iron expressed as FeO

observed in the phonolitic rocks (Figs. 4 and 5) and pyroxene phenocryst cores in the basanite have compositions which are similar to those of phenocrysts cores in kenytes and syenites (Fig. 5).

Olivine. Representative olivine analyses are presented in Table 2. The analyzed basanite contains olivine ranging in composition from Fo_{75}–Fo_{84}. Kenytes contain olivine with compositions ranging from Fo_{57}–Fo_{63} and these olivines are more Mg-rich than those in the hawaiites (Fo_{54}–Fo_{59}). In one of the kenytes (K33) the olivine shows a slight tendency to reverse zoning with the average core composition being $Fo_{60.6}$ (range 60.4–60.8) and the average rim composition being $Fo_{61.1}$ (range 60.7–61.6). The nepheline syenites show much more variation in olivine composition than the eruptive rocks. Olivine ranges in composition from Fo_{62} to Fo_{21} in the syenites and nepheline syenites. Phenocrysts of olivine are not common in the trachytes and feldspathoidal phonolites. In one feldspathoidal phonolite the olivine phenocrysts were found to have a uniform composition of Fo_{40}. The pantelleritic trachyte examined in this study contains fayalitic olivine with a composition of $Fo_{1.7}$.

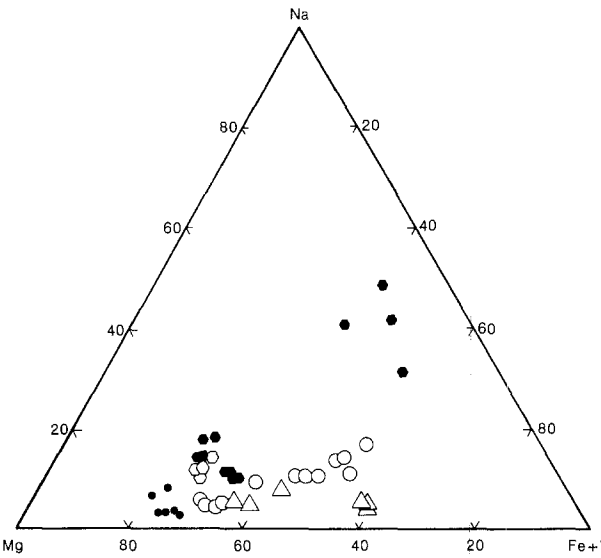

Fig. 4. Electron microprobe analyses of pyroxenes from Mt. Kenya plotted in terms of atomic Na-Mg-(Fe+Mn). Symbols as in Fig. 3. *Small closed circles* = basalts

Magnetite

In most of the samples examined as part of this study the dominant opaque mineral is homogeneous titanmagnetite. In some of the syenitic rocks the magnetite has been oxidized to ilmenite-magnetite intergrowths. Representative magnetite analyses are presented in Table 3. Magnetites in the kenytes have higher $MgAl_2O_4$ component than in most of the other samples and spinels in the basanite sample are high in $MgAl_2O_4$ and $MgCr_2O_4$ components.

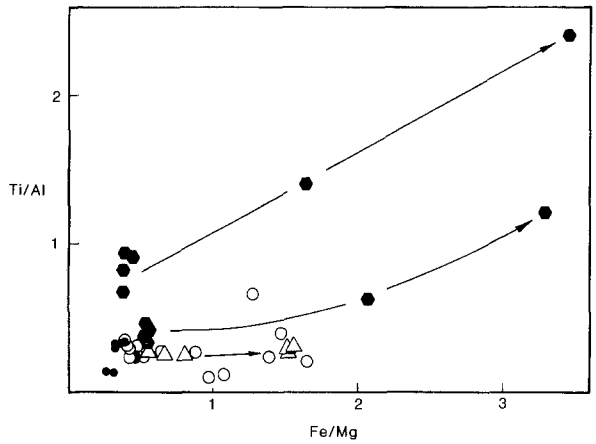

Fig. 5. Pyroxene analyses for Mt. Kenya volcanics and intrusives plotted in terms of atomic Ti/Al versus Fe/Mg. Arrows indicate changing compositions from core to rims to groundmass. Symbols as in Figs. 3 and 4

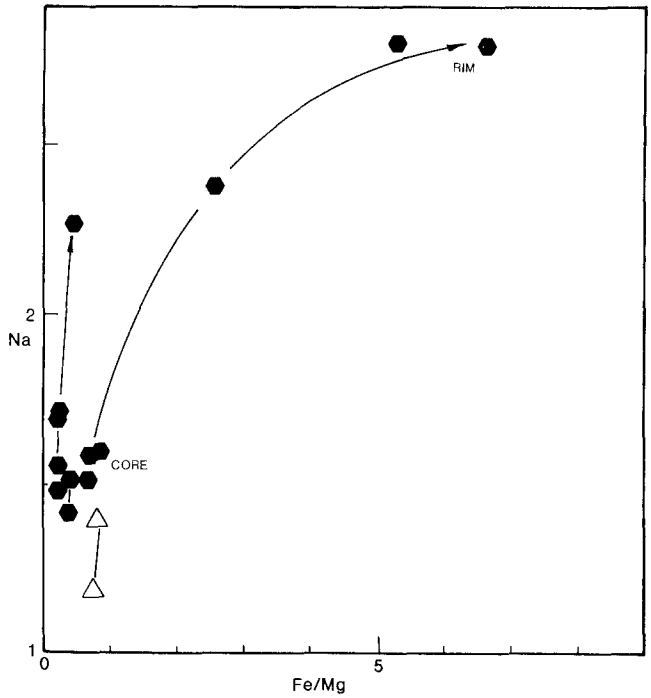

Fig. 6. Amphibole analyses for Mt. Kenya volcanics and intrusives plotted in terms of Na versus Fe/Mg showing compositional variation from core to rim in syenites. Symbols as in Fig. 3

Amphibole and aenigmatite

Aenigmatite occurs in most of the phonolites, feldspathoidal trachytes, trachytes, and syenitic rocks and some representative analyses of aenigmatite are presented in Table 4.

Alkali amphiboles occur in most of the syenitic rocks, in some of the phonolites and feldspathoidal trachytes and in the quartz-normative trachyte. The amphiboles are sodic-calcic and alkali varieties and range in composition from kataphorite-richterite group to arfvedsonite (using classification of Leake 1978). Among the phonolitic and syenitic rocks there is a trend of increasing Fe/Mg ratio and increasing Na content from cores to rims of amphiboles (Fig. 6). Most of the amphiboles are kataphorite-richterite types and some rocks contain amphiboles which are zoned to arfvedsonite rims. The quartz-normative trachyte contains an arfvedsonite amphibole. Amphiboles in the phonolitic and syenitic rocks are also zoned with respect to Al and Ti in the tetrahedral site. Rims of zoned crystals tend to be lower in Al^{IV} and Ti (Fig. 7). Representative analyses are presented in Table 5.

Geochemistry

Three main chemical groups

Two major groupings among the felsic rocks, and a third group consisting of the few mafic rocks we have analysed, are geochemically distinguishable (Tables 6, 7 and 8). Most of the felsic samples are moderately or strongly undersaturated (>10% normative nepheline) and will be referred to as the *phonolite suite*. This group contains all the samples from the main eruptive phase of the volcano as well as those of the central intrusive complex. The post-main-phase samples include a suite of five trachytes that are critically

Table 2. Representative olivine analyses

	1	2	3	4	5	6	7	8	9	10
	33	22	4	11	14	54	20	38N	38	51
SiO_2	36.70	34.96	36.30	31.79	32.04	32.88	29.25	37.88	39.91	35.78
FeO*	31.76	35.39	34.20	52.08	51.28	45.94	64.44	22.00	14.91	35.96
MnO	1.69	2.06	3.07	8.12	2.96	2.18	3.52	0.29	0.16	1.01
MgO	29.80	26.90	27.11	7.94	11.64	17.95	0.62	39.86	44.27	27.07
CaO	0.25	0.30	–	0.39	0.51	0.49	0.36	0.10	0.24	0.56
NiO	–	0.01	–	–	–	–	–	0.13	0.13	0.02
Total	100.20	99.62	100.68	100.32	98.43	99.44	98.19	100.26	99.62	100.40
	Structural formulae on basis of 32 oxygens									
Si	8.039	7.896	8.056	8.057	8.049	7.893	8.021	7.880	8.043	7.981
Fe	5.818	6.684	6.344	11.039	10.774	9.223	14.781	3.817	2.513	6.709
Mn	0.313	0.394	0.576	1.743	0.630	0.443	0.818	0.051	0.026	0.192
Mg	9.731	9.055	8.968	2.999	4.360	6.422	0.253	12.328	13.302	9.000
Ca	0.059	0.073	–	0.105	0.137	0.127	0.105	0.022	0.052	0.133
Ni	–	0.001	–	–	–	–	–	0.022	0.021	0.004
Fo%	62.6	57.5	58.6	21.4	28.8	41.0	1.7	76.4	84.1	57.3

Table 3. Representative spinel analyses

	1	2	3	4	5	6	7	8	9
	52	33	22	4	46	20	38N	38	51
TiO_2	14.28	21.62	23.64	20.31	24.03	24.82	1.54	20.48	22.12
Al_2O_3	0.19	2.09	1.75	0.19	0.54	1.68	44.43	6.27	2.40
FeO*	78.70	64.41	65.25	71.60	67.02	67.16	33.04	63.14	68.89
MnO	1.41	1.80	1.58	2.57	2.03	1.13	0.20	0.72	0.69
MgO	–	3.49	1.60	0.30	0.55	0.56	12.82	2.98	2.09
Cr_2O_3	–	–	0.06	0.09	0.04	0.04	8.10	2.70	0.05
SiO_2	–	0.71	–		–	–			
Total	94.58	94.12	93.88	95.06	94.21	95.39	100.13	96.29	96.24
	Structural formulae on basis of 24 cations and 32 oxygens								
Si		0.213							
Ti	3.305	4.876	5.458	4.695	5.609	5.696	0.261	4.466	4.940
Fe^{2+}	10.938	11.074	12.316	11.888	12.821	13.150	3.931	11.003	11.840
Fe^{3+}	9.320	5.083	4.436	6.517	4.574	3.994	2.277	4.307	5.268
Mn	0.368	0.457	0.411	0.669	0.534	0.293	0.038	0.176	0.174
Mg		1.558	0.730	0.138	0.254	0.253	4.292	1.287	0.927
Al	0.069	0.739	0.635	0.069	0.198	0.604	11.764	2.141	0.840
Cr		–	0.014	0.024	0.011	0.009	1.438	0.620	0.012

Table 4. Representative aenigmatite analyses

	1	2	3	4
Sample no:	52	4	11	14
SiO_2	41.07	41.86	40.14	39.77
TiO_2	5.44	9.35	8.80	9.31
Al_2O_3	0.99	1.96	1.59	1.26
FeO*	41.34	27.08	35.98	39.05
MnO	1.55	1.20	1.73	1.39
MgO	1.21	10.12	2.03	1.43
CaO	0.28	0.73	0.41	0.63
Na_2O	7.60	7.85	7.71	6.90
K_2O	0.09	0.01	0.12	0.04
Cr_2O_3		0.08		
NiO		0.09		
BaO		–		
Total	99.57	100.33	98.51	99.78
	Structural formulae on basis of 20 oxygens			
Si	5.974	5.636	5.779	5.717
Al	0.170	0.310	0.270	0.214
Ti	0.595	0.947	0.953	1.007
Cr		0.008		
Fe	5.030	3.049	4.333	4.694
Mn	0.191	0.137	0.211	0.170
Mg	0.263	2.031	0.437	0.307
Ni		0.009		
Ca	0.044	0.105	0.064	0.097
Na	2.144	2.050	2.153	1.923
K	0.016	0.001	0.022	0.007
Ba		–		

Table 5. Representative amphibole analyses

Sample	1	2	3	4	5	6	7
no:	4	4	11	14C	14R	46	20
SiO_2	49.93	54.33	50.34	48.33	49.82	49.11	48.54
TiO_2	3.47	1.81	2.07	2.45	0.45	1.37	1.23
Al_2O_3	3.60	0.80	3.62	3.49	0.66	3.89	0.52
FeO*	7.63	12.30	11.12	15.16	30.69	17.17	31.17
MnO	0.40	0.62	0.63	0.57	1.22	0.57	1.42
MgO	17.30	14.96	15.71	12.74	2.58	11.92	1.90
CaO	7.92	3.33	8.48	7.91	1.47	8.51	3.39
Na_2O	5.55	8.02	5.38	5.19	8.96	4.81	6.10
K_2O	1.28	1.31	1.29	1.35	1.59	1.47	1.07
Cr_2O_3	0.03	0.06	0.01				
NiO	0.07	–	0.05				
BaO	0.03	–	0.01				
Total	97.21	97.54	98.71	97.19	97.44	98.82	95.34
	Structural formulae on the basis of 22 oxygens and 2 OH group						
Si	7.234	7.901	7.299	7.263	7.996	7.312	7.963
Al^{IV}	0.614	0.099	0.618	0.618	0.004	0.682	0.037
Al^{VI}	–	0.038	–	–	0.121	–	0.064
Ti	0.378	0.198	0.226	0.277	0.054	0.153	0.151
Cr	0.004	0.006	0.001				
Fe^{2+}	0.925	1.496	1.349	1.906	4.119	2.137	4.277
Mn	0.049	0.076	0.077	0.073	0.165	0.072	0.197
Mg	3.737	3.243	3.395	2.855	0.618	2.645	0.465
Ni	0.008	–	0.005				
Ca	1.230	0.520	1.318	1.274	0.253	1.358	0.597
Na	1.559	2.262	1.512	1.512	2.789	1.388	1.941
K	0.236	0.243	0.240	0.259	0.325	0.279	0.225
Ba	0.002	–	0.001				

saturated with silica (<4% normative quartz, <4% normative nepheline). This critically saturated group will be termed the *trachyte suite*, and it excludes the post-main-phase phonolites which are part of the phonolite suite. Normative compositions for the phonolite suite plot along the thermal trough in the system Q–Ne–Ks, whereas the trachyte suite falls close to the thermal divide (Fig. 8).

A significant point to make with regard to this three-fold division of analysed Mount Kenya rocks, and, by implication, to the nature of their source rocks (see below),

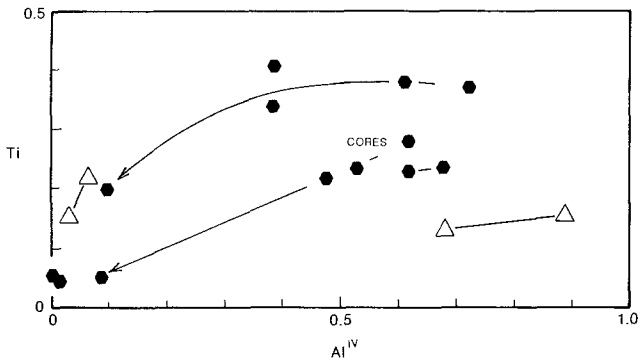

Fig. 7. Amphibole compositions for Mt. Kenya volcanics and intrusives plotted in terms of atomic Ti versus Al in tetrahedral sites. Symbols as in Fig. 3

is that the mafic and two felsic groups are indistinguishable on the basis of some incompatible trace-element ratios. For example, all of the samples of this study – including the mafic rocks, but with the exception of two altered phonolites – have similar Zr/Nb (3.68 ± 0.37 at 1σ) and Zr/Th (42 ± 7 at 1σ) values. Neither can the two felsic suites be distinguished on the basis of Zr/Rb values (Fig. 10). Zr/Hf values (Table 10), however, range from 58.3 to 65.0 for the phonolite suite, and are slightly lower for the trachyte suite (55).

Sr isotopes

Twenty-six whole-rock samples have been analysed for $^{87}Sr/^{86}Sr$ (Table 9). Initial ratios are in the range 0.70339–0.70380, and the majority of the phonolite-suite rocks have $^{87}Sr/^{86}Sr$ values in the narrow range 0.70360–0.70366, if an age of 3 My (Baker 1967; Baker et al. 1971) is assumed for all samples. The initial $^{87}Sr/^{86}Sr$ values for the Mount Kenya suite as a whole are similar to those of other alkalic volcanic rocks in continental and oceanic settings (e.g. Bell and Powell 1970; Laughlin et al. 1971; Price and Compston 1973; Rock 1976; White et al. 1979).

The trachyte-suite samples are clearly distinguishable isotopically from those of the phonolite suite and from the mafic rocks. Their range of initial $^{87}Sr/^{86}Sr$ values is 0.70349–0.70355, in contrast to the ranges of the other two groups which are consistently higher. The pantelleritic trachyte dyke sample has a $^{87}Sr/^{86}Sr$ value (0.70339) that is significantly lower than other values for the trachyte suite, assuming an age of 3 My. However, if it is assumed to have a ratio similar to the other analysed rocks of the trachyte suite (0.70355) then an age of 1.4 My is obtained.

The highest $^{87}Sr/^{86}Sr$ inital ratios are for samples of aphyric phonolites that represent some of the stratigraphically older material sampled as part of this study (Fig. 2): samples K40 and K52 are either distinctly radiogenic in comparison with the rest of the suite, or are significantly older. If these two samples are assumed to have the same initial $^{87}Sr/^{86}Sr$ (0.70362) as the other strongly and moderately undersaturated rocks of the suite, then K40 gives an age of 4.0 My and K52 one of 5.5 My.

Major and trace-element trends

The significant aspects of major and trace-element trends observed within the two felsic suites from Mount Kenya are presented graphically in Figs. 9 and 10. Rb has been chosen as the reference element in these diagrams because it has a wide range of values within the suites and is considered to partition strongly in favour of the melt in the magmas represented by these rocks. Samples believed to be related by crystal fractionation processes are indicated in Figs. 9 and 10 (see below).

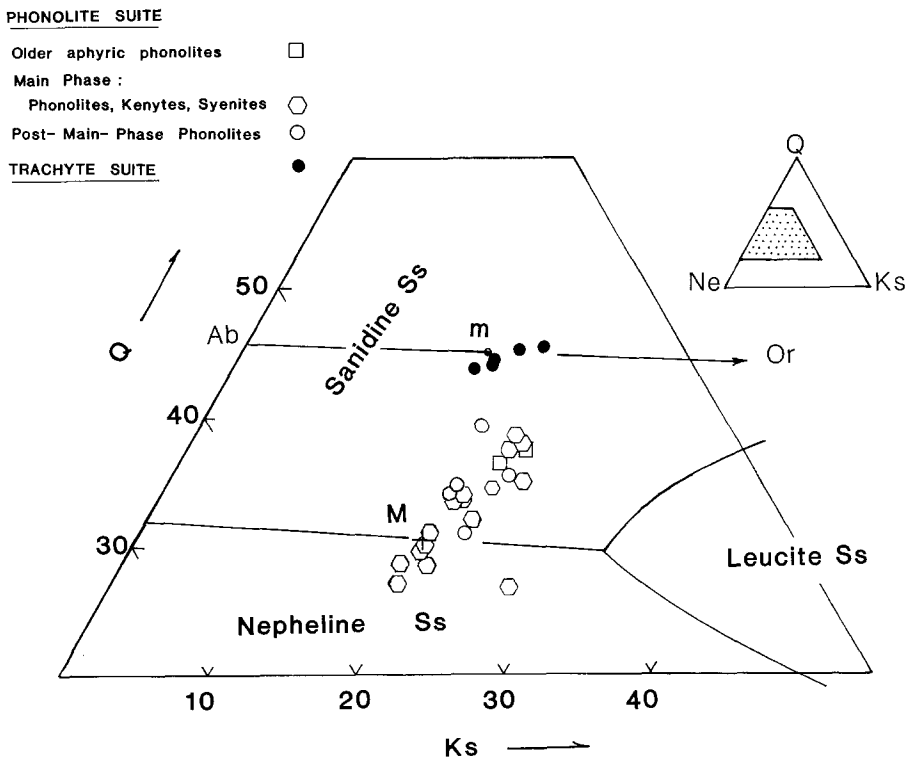

Fig. 8. Whole rock analyses of Mt. Kenya eruptives and intrusives plotted in the system Q-Ne-Ks. Phase relationships are from Hamilton and MacKenzie (1965): "m" represents the thermal minimum on the Ab-Or join and "M" the thermal trough on the Ne-sanidine phase boundary

Table 6. Representative analyses of eruptives and intrusives from the main eruptive phase

	1	2	3	4	5	6	7	8	9	10	11	12	13	14	15
Sample no:	47	15	52	40	18	4	9	33	22	39	45	26	8	11	14
SiO_2	53.98	56.80	52.66	58.13	51.70	52.09	52.15	52.39	52.40	53.43	53.63	53.64	54.24	56.34	56.47
TiO_2	1.32	0.82	0.25	0.27	1.05	1.43	0.83	1.16	1.39	0.73	0.90	0.89	0.79	1.15	0.95
Al_2O_3	18.79	18.37	19.90	15.94	19.12	18.45	19.50	19.20	18.56	20.05	19.33	19.03	19.48	18.33	17.86
Fe_2O_3	2.51	2.44	2.81	3.23	2.37	2.94	3.13	0.67	1.69	2.69	1.43	2.16	3.09	1.87	1.63
FeO	3.25	2.29	3.56	4.18	2.95	4.02	1.99	4.56	4.82	2.76	4.15	3.33	2.14	3.27	3.71
MnO	0.32	0.21	0.30	0.29	0.26	0.26	0.24	0.25	0.32	0.29	0.26	0.25	0.24	0.23	0.24
MgO	0.96	0.74	0.49	0.39	1.38	1.27	0.87	1.38	1.37	0.83	1.16	1.20	0.94	0.95	0.76
CaO	3.39	1.80	1.61	1.61	2.25	2.36	1.36	2.12	2.53	1.65	2.14	2.21	1.45	1.82	2.13
Na_2O	6.87	8.73	9.41	8.02	7.99	9.02	9.01	9.67	9.38	10.25	8.50	7.91	0.44	8.83	7.21
K_2O	5.01	5.18	5.87	5.68	4.76	4.93	7.19	5.44	5.04	5.03	5.65	5.48	4.77	5.35	5.35
P_2O_5	0.69	0.44	0.22	0.12	0.64	1.16	0.48	0.92	0.98	0.71	0.74	0.72	0.63	0.55	0.38
H_2O^+	1.53	1.20	1.29	1.18	3.02	0.83	1.50	1.77	0.65	0.81	1.10	1.20	0.92	1.13	1.72
H_2O^-	1.15	0.05	1.04	1.09	0.58	0.18	0.33	0.20	0.28	0.12	0.55	1.20	0.15	0.20	0.48
CO_2	0.20	0.07	0.08	–	1.21	–	1.12	0.03	0.62	0.01	0.16	0.17	0.05	0.07	0.69
S	0.07	0.07	0.05	0.04	0.05	0.03	0.07	0.07	0.07	0.04	0.05	0.06	0.05	0.05	0.05
F	0.13	0.22	0.19	0.15	0.29	0.44	0.36	0.30	0.25	0.17	0.14	0.32	0.44	0.24	0.27
Total	100.17	99.43	99.73	100.32	99.62	99.41	100.13	100.13	100.35	99.57	99.89	99.77	99.82	100.38	99.90
$O \equiv F, S$	0.09	0.13	0.11	0.08	0.15	0.20	0.19	0.16	0.14	0.09	0.08	0.16	0.21	0.13	0.14
Total	100.08	99.30	99.62	100.24	99.47	99.21	99.94	99.97	100.21	99.48	99.81	99.61	99.61	100.25	99.76
	Trace elements (concentrations in ppm)														
Rb	113	119	140	136	117	130	180	146	137	169	186	171	172	126	111
Ba	1,241	1,755	160	214	1,200	1,116	763	1,082	1,323	931	845	907	759	1,381	1,618
Sr	1,043	859	79	52	1,762	1,088	435	1,008	1,084	445	526	577	458	548	750
Pb	8	6	11	17	9	6	10	9	11	7	8	9	6	7	11
Th	17	18	16	19	34	24	18	29	33	28	35	32	27	18	13
U	1	2	3	4	6	3	7	5	6	6	4	2	7	3	5
La	121	64	107	197	96	108	90	100	127	136	115	106	89	103	112
Ce	208	169	158	325	162	176	134	144	219	207	168	175	121	172	187
Y	41	35	33	61	35	35	28	33	43	43	41	34	42	38	38
Zr	779	850	638	848	1,413	913	705	1,118	1,323	1,064	1,238	1,139	1,019	920	800
Nb	193	244	165	296	387	262	369	299	358	293	329	325	332	269	237
Sc	6	3	4	3	3	3	3	4	4	3	4	3	3	4	3
V	38	21	8	4	28	41	15	30	39	16	24	24	21	27	25
Ni	<1	<1	1.5	<1			1.1	<1	<1	1.3	<1	1.2	1.6	<1	<1
Cu	16	11	12	4	10	14	5	12	12	17	12	13	10	9	12
Zn	119	112	171	183	123	114	124	125	151	140	138	132	124	112	124
Ga	21	23	24	27	20	20	27	20	21	23	21	21	33	25	24
F	1,333	2,229	1,919	1,465	2,867	4,440	3,644	3,037	2,519	1,743	1,438	3,242	4,403	2,390	2,655

Analyses for major elements by XRF using techniques of Norrish and Hutton (1969). Na by flame photometry, FeO by a titration technique, H_2O and CO_2 by gravimetric method. Trace elements by XRF using methods described by Norrish and Chappell (1967), except for F which is determined by specific ion electrode.

Explanation: 1, 5, 8, 9 Kenytes; 2, 3, 4, 10, 11, 12 Phonolites and trachytes; 6, 7, 13, 14, 15 Nepheline syenites and syenites

The trachyte suite is a chemically coherent set of samples whose data define smooth major element trends relative to Rb. FeO (total), MgO, CaO, and P_2O_5 values decrease and Na_2O+K_2O values increase, as Rb abundances increase (Fig. 9). The trachyte suite is distinguished from the phonolite suite particularly by its lower Na_2O+K_2O values (Fig. 9). The phonolite suite is geochemically much less coherent than the trachyte suite. For example, at a given Rb abundance there is a much broader range of FeO (total), CaO, and Na_2O+K_2O. MgO increases slightly with increasing Rb within most of the phonolite suite, although one sample (K55) is relatively depleted in MgO. In addition, there is considerable scatter on the P_2O_5 versus Rb diagram, caused by several of the high Rb members of the phonolite suite having very high P_2O_5 abundances.

Trace elements in the trachyte suite also define smooth trends: Sr, Ba and V decrease as Rb increases, and Zr, Th, Y, La, Ce and Ga increase (Fig. 10 and Table 8). The Ba/Sr values increase as Rb increases (Fig. 11), and Rb/Cs is very high in the most fractionated trachytes (Table 10). The phonolite suite is distinguished from the trachyte suite by the relative abundance levels of Ba, Sr, Y and V, but trace element differences are considerably less systematic in the phonolite suite. For example, Ba decreases systematically as Rb increases, but the later phonolites and older aphyric phonolites have values that are distinctly different from those shown by the main phase phonolites, nepheline syenites and kenytes (Fig. 10). In addition, the range of Sr is wide in the phonolite suite. The kenytes and some of the syenites are higher in Sr that are most of the other

Table 7. Representative analyses of later eruptives

	1	2	3	4	5	6	7	8	9	10	11
Sample no.	23	46	54	55	35	36	20	38	49	34	51
SiO_2	53.80	55.74	55.96	57.28	57.99	58.28	65.04	41.43	46.17	47.79	50.07
TiO_2	1.17	0.85	0.92	0.24	0.81	0.81	0.22	3.64	2.98	2.28	2.23
Al_2O_3	15.84	18.26	17.63	18.15	16.37	15.99	15.77	11.87	15.54	16.16	16.37
Fe_2O_3	7.42	1.51	1.80	2.04	1.31	1.69	0.90	2.74	2.35	2.75	1.63
FeO	3.46	4.63	5.40	4.16	7.34	7.11	2.84	11.55	10.52	7.18	9.32
MnO	0.34	0.25	0.23	0.26	0.31	0.31	0.17	0.23	0.28	0.24	0.25
MgO	1.30	1.01	0.78	0.27	0.82	0.74	0.15	10.52	4.31	5.45	2.93
CaO	3.60	2.57	3.33	1.84	2.76	2.79	0.99	11.10	7.48	6.69	5.96
Na_2O	6.27	8.53	7.15	7.95	6.63	6.69	6.98	2.33	4.77	5.16	5.71
K_2O	3.49	4.82	4.58	5.92	4.14	4.16	5.57	1.48	2.38	2.13	2.74
P_2O_5	0.75	0.41	0.54	0.19	0.51	0.51	0.10	0.94	1.67	0.68	1.18
H_2O^+	0.50	0.36	0.60	0.56	0.38	0.27	0.49	0.87	0.81	1.53	0.28
H_2O^-	0.51	0.38	0.15	0.38	0.27	0.16	0.11	0.70	0.58	1.31	0.25
CO_2	1.81	0.02	0.18		0.10	0.01	0.07	0.07	0.06	0.01	0.89
S	0.04	0.04	0.05	0.04	0.04	0.05	0.04	0.01	0.07	0.05	0.05
F	0.07	0.15	0.14		0.26	0.12	0.36				
Total	100.37	99.53	99.44	99.28	100.04	99.69	99.80	99.48	99.97	99.41	99.86
$O \equiv F, S$	0.05	0.08	0.08	0.02	0.13	0.08	0.17		0.04	0.03	0.03
Total	100.32	99.45	99.36	99.26	99.91	99.61	99.63	99.48	99.93	99.38	99.83
	Trace elements (concentrations in ppm)										
Rb	59	94	91	174	96	88	168	52	29	43	56
Ba	1,383	1,324	1,111	402	1,228	1,337	236	622	912	656	1,028
Sr	647	881	573	66	482	481	26	1,230	1,672	906	1,375
Pb	4	12	3	15	15	11	29	4	8	6	8
Th	8	15	14	24	14	13	39	5	8	11	5
U	<1	<1	2	6	2	2	2	<1	<1	3	1
La	97	107	79	122	72	96	228	73	80	78	81
Ce	151	167	130	165	156	161	314	100	158	113	149
Y	44	33	36	45	40	44	88	26	33	30	29
Zr	385	545	542	876	614	545	1,119	197	315	487	283
Nb	101	145	135	197	137	127	301	59	92	141	86
Sc	14	3	5	2	7	7	2	22	13	15	9
V	17	23	26	5	23	14	<1	350	165	188	113
Ni	<1	<1	1.3	1.2	<1	<1	<1	137	7.5	92	2.0
Cu	15	11	18	13	15	14	7	84	42	61	38
Zn	125	107	109	165	125	111	157	100	109	109	113
Ga	18	21	23	26	24	22	30	16	15	16	18
F	714	1,455	1,412		2,555	1,164	3,564				

Explanation: 2, 3, 4, 5, 6 Feldspathoidal trachytes and phonolites; 1, 7 Quartz-normative trachytes; 8, 9, 10, 11 Mafic rocks

phonolite suite samples and the later phonolites and earlier aphyric phonolites have lower abundance levels for Sr than do the main phase members of the phonolite suite at equivalent Rb abundance.

Ga abundances are similar for most members of the phonolite suite (18–24 ppm) but some high-Rb samples have high Ga abundance (up to 34 ppm). Y tends to increase slightly as Rb increases, and the range of V values in the phonolite suite is exceptionally wide; from less than 20 ppm up to greater than 40 ppm (the kenytes and some syenites have the highest V values, whereas later phonolites and earlier aphyric phonolites have the lowest V abundances).

Ba/Sr values are generally less than 3 for the phonolite suite, and those for the kenytes are around 1 (Fig. 11). One late stage phonolite and one early aphyric phonolite have Ba/Sr values significantly higher than the rest of the phonolite suite. Five samples of the phonolite suite have been analyzed for Cs (Table 10), and in these Rb/Cs values decrease as Rb abundances increases.

Rare earth element chemistry

Rare earth analyses for three main phase phonolitic rocks (one kenyte and two nepheline syenites), two post-main phase phonolites and two samples of the trachyte suite are presented in Table 10. Chondrite normalized rare earth patterns are presented in Fig. 12.

The phonolite suite samples all show similar patterns characterized by light rare earth enrichment and flat heavy rare earth patterns. Eu anomalies are absent for these samples and abundance levels are similar. One of the trachytes (K35) has a pattern very similar to those of the samples from the phonolite suite with the only differences being slightly lower light rare earth abundance and slightly higher heavy rare earth abundance. The other trachyte sample

Table 8. CIPW Norms for Representative Mt. Kenya Alkalic Rocks

	1	2	3	4	5	6	7	8	9	10	11	12	13	14	15
Sample no.	K49	K51	K4	K33	K22	K39	K26	K1	K8	K11	K55	K54	K46	K35	K20
Q															3.88
Or	14.12	16.19	29.14	32.15	29.79	29.73	32.39	32.62	28.19	31.62	34.99	27.07	28.49	24.47	32.92
Ab	23.56	37.23	22.32	21.01	24.12	21.55	30.57	19.76	25.47	31.59	28.81	39.80	30.47	49.35	50.11
An	13.22	10.95					0.24					2.49		2.68	
Ne	9.88	6.01	24.45	25.71	23.45	29.03	19.70	26.03	26.09	17.83	17.11	11.22	19.84	3.66	
Ac			7.81	1.94	4.89	7.78		10.10	8.94	5.41	5.90		4.37		2.60
Di	5.25	1.79	1.42	1.34	0.68	1.05	2.12	0.75	1.09	1.60	0.64	1.90	2.37	1.03	0.26
He	5.54	2.66	2.05	2.31	1.21	1.91	1.98	0.99	1.21	2.62	6.30	6.18	6.15	5.10	3.10
En															0.25
Fs															3.44
Fo	5.99	4.53	1.76	1.97	2.17	1.11	1.41	1.36	1.29	1.14	0.26	0.74	0.99	1.10	
Fa	7.99	8.52	3.21	4.29	4.91	2.55	1.66	2.25	1.80	2.35	3.31	3.05	3.25	6.83	
Mt	2.94	2.36	0.35				3.13					2.61		1.90	
Il	5.77	4.24	2.72	2.20	2.64	1.39	1.69	1.37	1.50	2.18	0.46	1.75	1.61	1.54	0.42
Ap	4.00	2.74	2.70	2.14	2.28	1.65	1.67	1.44	1.46	1.28	0.44	1.26	0.95	1.19	0.23
Py	0.07	0.09	0.06	0.13	0.13	0.07	0.11	0.07	0.09	0.09	0.07	0.09	0.07	0.07	0.07
CC	0.23	2.02		0.07	1.41	0.02	0.39	0.30	0.11	0.16		0.41	0.05	0.23	0.16
Ns				2.59	1.49	0.64		1.32	1.06	0.95	0.04		0.03		1.40
H_2O	0.77	0.53	1.01	1.97	0.93	0.93	2.40	1.26	1.07	1.33	0.94	0.75	0.74	0.65	0.60

Explanations: 1 Ne-hawaiite; 2 Ne-mugearite; 3 Ne-syenite; 4, 5 Kenytes; 6, 7 Phonolites; 8, 9, 10 Nepheline syenites; 11 Post-main phase phonolite; 12, 13 Post-main phase phonolites; 14, 15 Trachytes

Table 9. Strontium isotopic compositions

Sample no.[a]	Rb	Sr	$Sr^{87/86}$	Initial $Sr^{87/86} \pm 2\sigma$*[b]
Main phase (phonolite suite)				
52	140	79	0.70402	0.70380±3
40	136	52	0.70405	0.70373±4
18	117	1,762	0.70366	0.70365±3
53	160	1,007	0.70367	0.70365±3
26	171	577	0.70369	0.70365±3
33	146	1,008	0.70364	0.70362±3
4	130	1,088	0.70363	0.70362±3
8	172	458	0.70370	0.70365±2
2	145	380	0.70364	0.70359±3
1	158	422	0.70369	0.70364±2
10	141	199	0.70375	0.70366±3
11	126	548	0.70367	0.70364±2
14	111	750	0.70363	0.70361±3
9	180	435	0.70366	0.70361±3
39	169	445	0.70368	0.70363±2
Post-main phase (including trachyte suite*)				
23	59	647	0.70356	0.70355±3*
25	93	432	0.70358	0.70355±3*
54	91	573	0.70362	0.70360±2
46	94	881	0.70366	0.70365±3
55	174	66	0.70395	0.70363±3
35	96	482	0.70352	0.70349±3*
36	88	481	0.70358	0.70355±3*
20	168	26	0.70392	0.70339±4*
Mafic suite				
49	52	1,672	0.70368	0.70368±2
34	29	906	0.70359	0.70359±3
51	56	1,375	0.70363	0.70362±6

[a] Samples are tabulated in stratigraphic order from oldest to youngest. Refer to Tables 6 and 7 for rock types

[b] Assuming an age of 3 My. Data relative to SRM 987 at 0.71032±2

(K20) has much higher total rare earth content than all the other samples and is characterized by a distinctive negative europium anomaly.

Discussion

A feature of other East African volcanic suites is that each is characterized by a constant ratio of Zr/Nb (Weaver et al. 1972, Lippard 1973) and this could imply specific mantle sources for each of the suites. The Mt. Kenya suite shows this feature with Zr/Nb, Zr/Th, and to some extent Zr/Rb ratios being reasonably constant for all rocks. However, within the Mt. Kenya sample set examined as part of this study two distinct suites characterized by different initial $^{87}Sr/^{86}Sr$ ratios are clearly distinguishable. The petrogenetic problems are: (a) to interpret geochemical variation within each suite; i.e. the phonolite suite and trachyte suite and (b) to relate the two suites to a mafic parental magma and to a mantle source.

Relationships within the phonolite suite

It is clear from the variability in abundance patterns for trace elements in the phonolite suite that no single liquid line of descent can explain all the variation within the suite. Among the post-main phase phonolites, and among the early aphyric phonolites are samples characterized by strong relative depletion in MgO, CaO, P_2O_5, Ba, Sr, and V; moderate to strong relative enrichment in Rb, Zr, Th, Y, La, Ce and Ga; and high Ba/Sr ratios and these rocks represent magmas derived by crystal fractionation from less evolved, moderately nepheline-normative phonolites. For example, phonolite K55 could be derived by crystal fractionation involving plagioclase, alkali-feldspar, clinopyroxene, magnetite and olvine from phonolite K54. Mathematical modelling (Wright and Doherty 1970) of this process for the major elements is presented in Table 11. Quantitative modelling of the trace elements (e.g. Zielinski and Frey

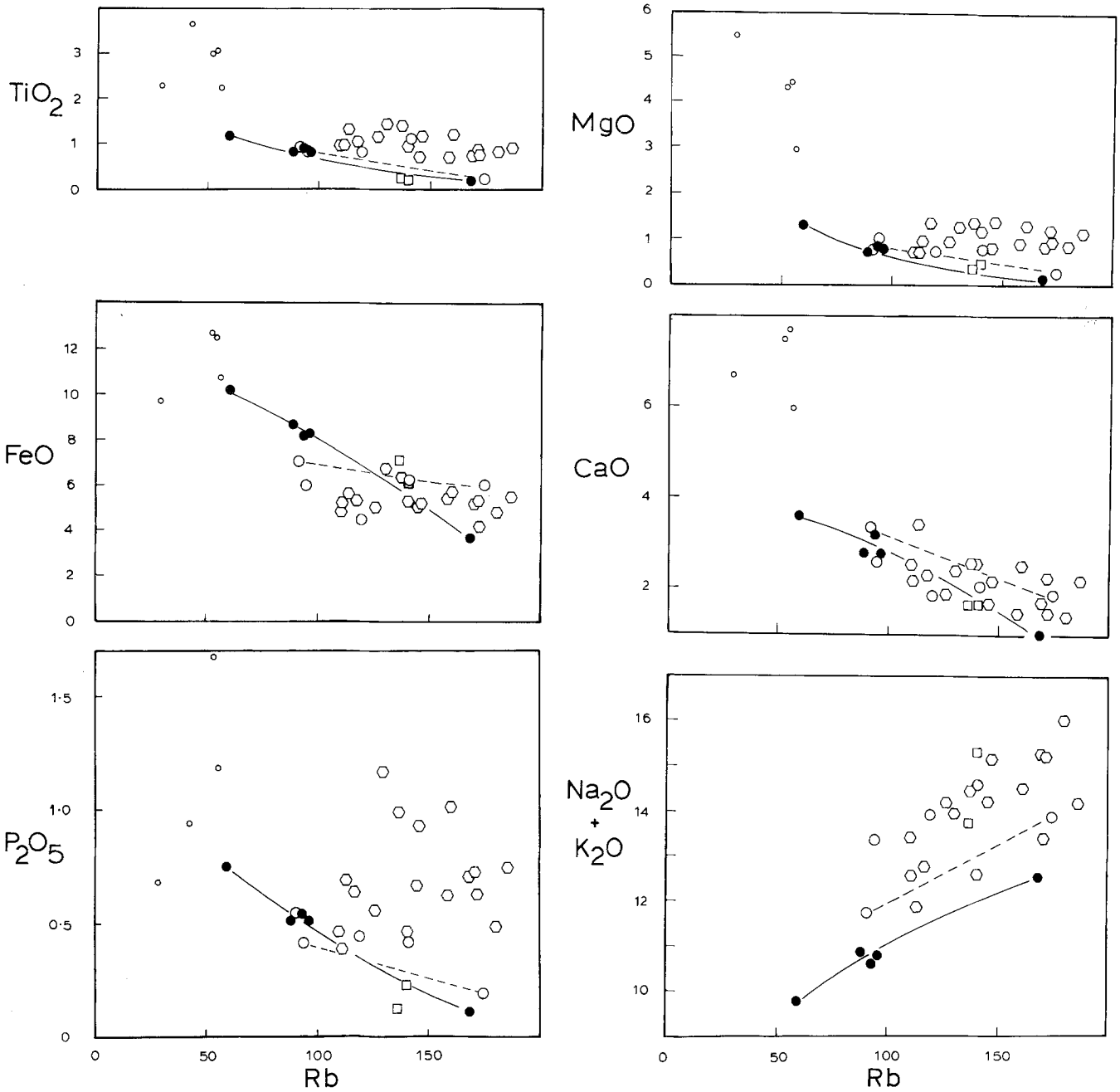

Fig. 9. Variation of selected major and minor elements (wt%) relative to Rb (ppm). Small open circles represent basalt analyses other symbols are as in Fig. 8. Lines represent examples of possible crystal fractionation paths for the phonolite suite (*broken line*) and trachyte suite (*unbroken line*)

1970) is subject to considerable uncertainity because the model involves large quantities of feldspar. Drake and Weill (1975) have demonstrated that plagioclase/melt distribution coefficients are temperature dependent and melt composition dependent. There is uncertainty regarding the validity of extrapolating Drake and Weill data to temperatures appropriate to phonolites and the temperature and melt composition dependence of alkali-feldspar/melt distribution coefficients is not known. In qualitative terms the derivation of K55 from K54 by a crystal fractionation model involving plagioclase, alkali-feldspar, clinopyroxene, magnetite and olivine is consistent with the trace element geochemistry.

K55 is an example of a member of the phonolite suite showing extreme depletion in Sr relative to Ba (Ba/Sr = 6.09) as a consequence of plagioclase fractionation. Most of the phonolites and nepheline syenites do not show these high Ba/Sr ratios and cannot be modelled in this way. High Na_2O+K_2O may suppress plagioclase crystallization in strongly undersaturated melts so that the crystal fractionation process is dominated by alkali-feldspar rather than plagioclase. As an example consider sample K8, a microsyenite with a Ba/Sr ratio of 1.66. K8 could be derived from the syenite K11 by crystal fractionation involving alkali-feldspar, clinopyroxene and spinel as illustrated by the mathematical model for this process presented in Table 11. The trace element chemistry is consistent with the model. Rb increases while Sr and Ba decrease and the Ba/Sr ratio should increase slightly. An attempt to model the trace elements Rb, Sr and Ba is included in Table 11.

The kenytes and two low-SiO_2 syenites of the phonolite

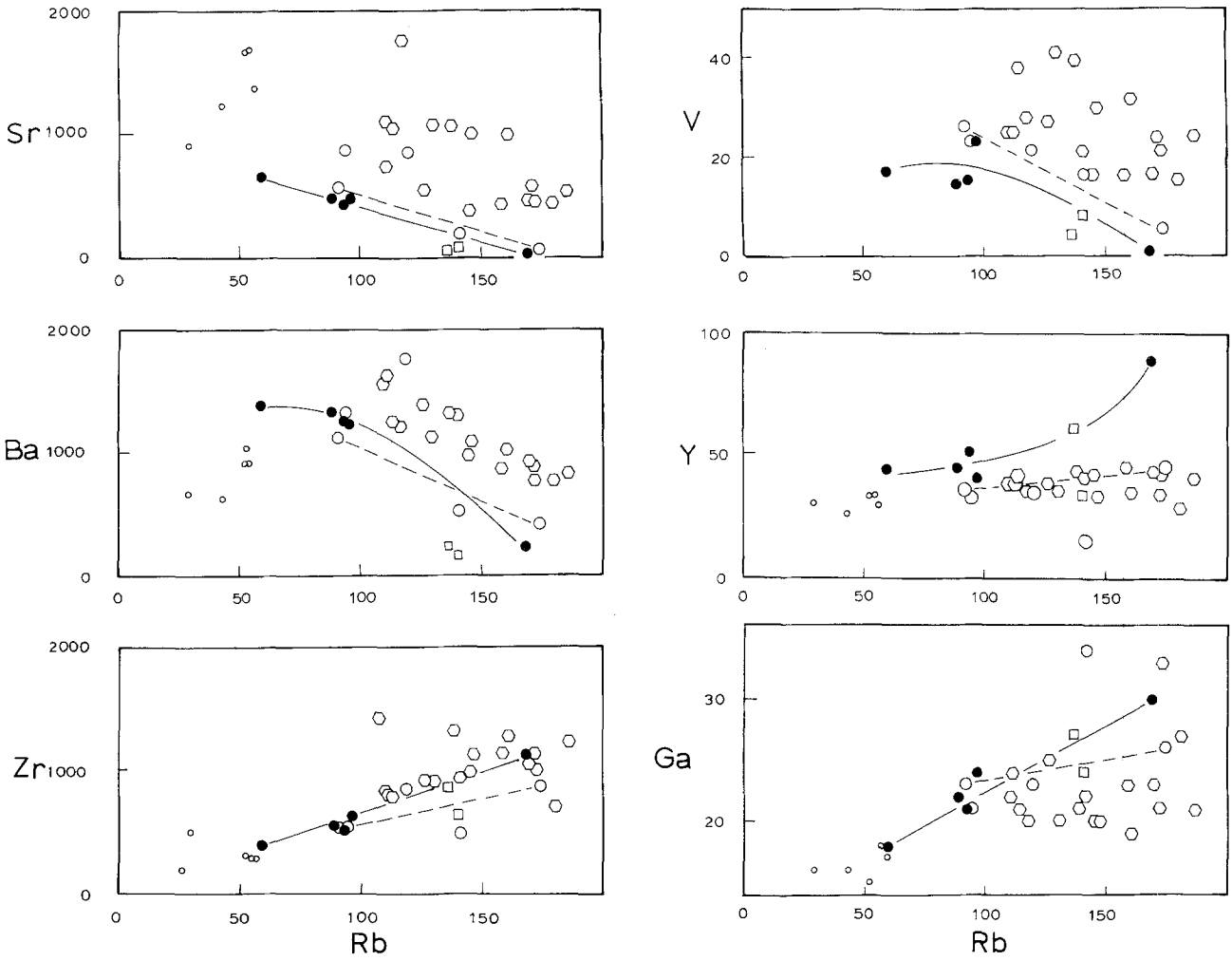

Fig. 10. Variation of selected trace elements versus Rb. Symbols as on Fig. 9

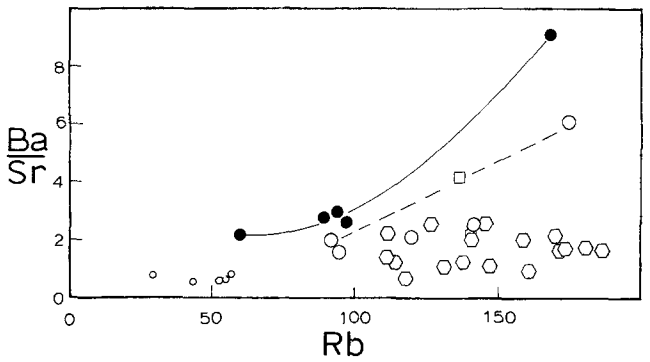

Fig. 11. Ba/Sr ratio versus Rb for the Mt. Kenya whole rock analyses. Symbols are as in Fig. 9

suite present a difficult petrogenetic problem because they cannot be simply related to the other members of the suite. The rocks which present a problem are characterized by the highest Zr, Nb and Th abundances in the suite and some of the highest Rb values. They are among the most strongly undersaturated rocks of the suite. On these grounds they might be considered to be extreme crystal fractionates derived from the other phonolites. However, they are also characterized by relatively high MgO, TiO_2, Na_2O and in some cases P_2O_5, and by higher Sr, V and in some cases Ba than other members of the phonolite suite with equivalent Rb contents. They are not cumulates because this is not consistent with high Zr, Nb and Rb abundances and relatively low SiO_2. Crystal fractionation involving alkali feldspar alone could explain the combination of high Zr and relatively high MgO but this is inconsistent with the Sr abundances and the lack of Eu anomalies in

Table 10. INAA for rare earth elements, Hf, and Cs on selected Mt. Kenya samples. Analysis of G-2 is provided as an indication of accuracy

	1	2	3	4	5	6	7	8
	K33	K4	K11	K46	K54	K35	K20	G2
La	85.6	95.7	93.3	95.0	80.9	64.8	236	90.1
Ce	167	194	188	183	159	158	390	168
Nd	56	71	68	66	58	59	126	53.1
Sm	8.8	11.3	11.1	10.5	9.4	10.2	18.8	7.15
Eu	2.70	3.30	3.89	3.43	2.90	3.07	1.07	1.36
Tb	1.30	1.40	1.34	1.26	1.27	1.22	2.37	0.46
Yb	4.63	4.27	4.54	3.89	3.86	5.50	11.0	0.68
Lu	0.75	0.68	0.70	0.57	0.60	0.84	1.08	0.11
Cs	2.2	1.6	1.2	0.8	0.7	1.0	0.3	1.29
Hf	17.2	14.6	15.6	9.3	9.3	11.1	20.7	7.62
Rb/Cs	66.4	81.3	105.0	117.5	130.0	96.0	560.0	
Zr/Hf	65.0	62.5	59.0	58.6	58.3	55.3	54.1	

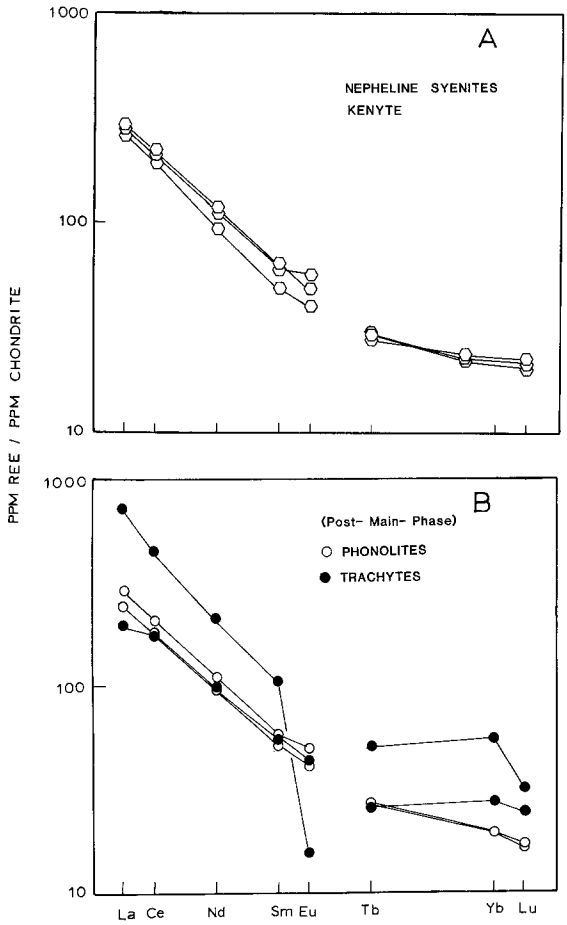

Fig. 12. Chondrite normalized rare earth element patterns for Mt. Kenya alkalic rocks

the rare earth patterns. The kenytes and low-SiO_2 syenites analyzed as part of this study cannot therefore be considered to have derived from other members of the phonolite suite.

Derivation of phonolite-suite magmas from more mafic magmas

The less evolved phonolites such as K54 and K46 with low Rb contents relative to the rest of the phonolite suite could be derived by crystal fractionation from basaltic parents. For example, K54 could be derived from the nepheline mugearite K51 by a crystal fractionation process involving plagioclase, clinopyroxene, magnetite and olivine (Table 12). Trace element modelling for this process is presented in Table 12. The fit for Rb is reasonable but Sr and Ba values are high. However, the trends in Sr and Ba are in the right direction and given the uncertainity of the partition coefficients this model gives an acceptable solution for the three trace elements selected.

The low-SiO_2 nepheline syenites and kenytes of the phonolite suite cannot be derived from the other phonolites. Attempts to model derivation of these rocks from basaltic parents by crystal fractionation are only moderately successful and give poor solutions for Na_2O and high total residuals. One of these models is presented in Table 12. The models are extremely sensitive to the choice of parental composition and the problem could be that the basanitic parental materials for the kenytes and high-SiO_2 syenites

Table 11. Models for evolution of phonolites and syenites; Mt. Kenya.

A: Feldspathoidal trachyte (K54)-phonolite (K55)

	K55		K54	Plag	Kspar	Cpx	Spinel	Olivine
	Calculated	Measured						
SiO_2	58.72	58.66	57.47	59.01	66.75	51.76		33.98
TiO_2	0.27	0.25	0.94			0.71	26.08	
Al_2O_3	18.44	18.59	18.11	25.90	18.94	1.76	0.59	
FeO	6.14	6.14	7.21	0.26	0.29	11.35	72.74	47.47
MgO	0.18	0.28	0.80			11.26	0.60	18.55
CaO	1.80	1.88	3.42	7.37	0.15	22.27		
Na_2O	8.28	8.14	7.34	6.68	6.85	0.84		
K_2O	5.72	6.06	4.70	0.78	7.01	0.05		

$\Sigma r^2 = 0.178$

Fraction of liquid remaining	0.711	Proportions of phases removed				
		45.9%	25.3%	17.9%	9.5%	1.4%

B: Syenite (K11) – microsyenite (K8)

	K8		K11	Kspar	Cpx	Spinel
	Calculated	Measured				
SiO_2	55.47	55.40	57.20	66.00	52.37	
TiO_2	1.10	0.81	1.17		0.45	25.52
Al_2O_3	19.81	19.90	18.61	18.87	0.94	0.57
FeO	4.92	5.03	5.03	0.36	11.23	71.17
MnO	0.25	0.25	0.23		0.67	2.16
MgO	0.74	0.96	0.96		11.51	0.58
CaO	1.49	1.48	1.85		21.15	
Na_2O	10.62	10.66	8.96	5.84	1.67	
K_2O	4.60	4.87	5.43	8.93	0.01	
P_2O_5	0.79	0.64	0.56			

$\Sigma r = 0.255$

Fraction of liquid remaining	0.702	Proportions of phases removed		
		82.4%	12.7%	5.0%

Trace elements

	K11	K8 (Calc.)		K8	
		Equilibrium model	Rayleigh model	Measured	Diff.
Rb	126	136	138	172	−19.8%
Sr	548	386	333	458	−15.7%
Ba	1,381	626	330	759	−17.5%
Ba/Sr		1.62	0.99	1.66	

Partition coefficients used in model

	Rb	Sr	Ba
Ksp	0.90	2.90	6.12
Cpx	0.0152	0.154	0.0128

Table 12. Models for Evolution of Phonolites from Basaltic Parents

A: Nepheline Mugearite (K51) → Feldspathoidal trachyte (K54)

	K54		K51	Plag	Cpx	Spinel	Olivine
	Calculated	Measured					
SiO_2	57.33	57.47	51.73	57.45	51.76		36.21
TiO_2	1.46	0.94	2.30		0.71	23.16	
Al_2O_3	18.29	18.11	16.91	25.72	1.76	2.51	
FeO	7.02	7.21	11.15	0.67	11.35	72.14	36.39
MgO	1.24	0.80	3.03		11.26	2.19	27.40
CaO	3.58	3.42	6.16	8.93	22.27		
Na_2O	7.71	7.34	5.90	6.56	0.84		
K_2O	5.05	4.70	2.83	0.67	0.05		
Σr^2 0.830							

Fraction of liquid remaining	0.532	Proportions of phases removed			
		58.5%	17.6%	13.7%	10.2%

	K51	K54 (Calc.)		K54	
		Equilibrium Model	Rayleigh Model	Measured	Diff.
Rb	56	104	104	91	+14.3%
Sr	1,375	994	820	573	+73.5%
Ba	1,028	1,498	1,570	1,111	+34.8%
Ba/Sr		1.51	1.91	1.94	

Partition Coefficients used in model

	Rb	Sr	Ba
Plag.	0.017	3.06	0.56
Cpx	0.0152	0.154	0.0128

B: Nepheline hawaiite (K49) → Nepheline syenite (K4)

	K4		K49	Plag	Cpx	Spinel	Olivine
	Calculated	Measured					
SiO_2	53.93	53.99	47.39	57.45	48.54		38.43
TiO_2	0.60	1.48	3.15		1.67	23.00	
Al_2O_3	19.49	19.12	16.12	25.72	7.77	2.50	
FeO	7.19	6.91	12.94	0.67	6.45	71.62	22.77
MnO	0.42	0.27	0.28		0.14	0.72	
MgO	1.22	1.32	4.57		13.04	2.17	38.80
CaO	2.55	2.45	7.95	8.93	21.42		
Na_2O	8.23	9.35	5.12	6.56	0.96		
K_2O	5.78	5.11	2.48	0.67			
Σr^2 2.739							

Fraction of liquid remaining	0.398	Proportion of phases removed			
		40.9%	36.6%	18.35%	4.13%

	K49	K4(Calc)		K4	
		Equilibrium model	Rayleigh model	Measured	Diff.
Rb	54	124	128	130	−4.6%
Sr	1,679	1,217	939	1,088	+11.9%
Ba	912	1,544	1,707	1,116	+38.4%
Ba/Sr		1.27	1.82	1.03	

Partition Coefficients used in model

	Rb	Sr	Ba
Plag	0.138	3.86	0.77
Cpx	0.0152	0.154	0.0128
Oliv	0.001	0.003	0.005

are not represented in the sample set. The broad range in composition represented within the phonolite suite reflects a range in parental magma compositions in terms of Na_2O+K_2O, MgO, TiO_2, P_2O_5, Ba, Sr, and Zr and this could be source related.

The evolution of the trachyte suite

The trachyte suite shows major and trace element variation that is consistent with crystal fractionation controlled by clinopyroxene and spinel with olivine and plagioclase at the less fractionated end and feldspar with spinel and possibly fayalitic olivine and amphibole for the strongly fractionated end members of the suite. Baker et al. (1977) in a study of the basalt-benmoreite-trachyte suite rocks of the southern part of the Gregory Rift in Kenya have rigorously tested crystal fractionation models for the evolution of trachytes and the geochemical trends observed in the trachyte suite from the summit of Mt. Kenya are similar. Quantitative mathematical models for the trachytes are very sensitive to mineral compositions used and such modelling requires more detailed mineral chemical information than presently available for the small number of trachyte suite samples represented in our sample set.

Sources for Mt. Kenya magmas

Norry et al. (1980) observed that in the north Kenya Rift there is a general trend towards silica saturation with time, and this trend is accompanied by decreasing incompatible element contents. They proposed that recent metasomatism of the mantle beneath Kenya by CO_2-rich fluids could be responsible for the trends observed. The Mt. Kenya sample suite reflects the regional pattern. Although crystal fractionation has played an important role in the evolution of the felsic rocks two aspects of the problem require a source related explanation. (a) The trachyte suite has a lower $^{87}Sr/^{86}Sr$ initial ratio and is critically saturated in contrast to the phonolite suite. (b) Within the phonolite suite, although $^{87}Sr/^{86}Sr$ initial ratios, Zr/Nb, Zr/Hf and Zr/Th ratios are constant, abundance levels for Ti, Mg, P, Sr, Ba, Zr and Nb vary over a wide range.

The variation in trace and minor element compositions within the phonolite suite is in part source related and in part related to the crystal fractionation processes involved in the evolution of the magmas represented. For example, extreme variation in Sr abundance in the strongly undersaturated phonolitic rocks is largely a consequence of the dominance or otherwise of feldspar in the crystal fractiona-

tion process. Those phonolitic rocks with low Sr (e.g. K55, Sr = 66 ppm) contrast strongly with low-SiO_2 phonolitic rocks with relatively high Sr (e.g. K33, Sr = 1,008 ppm) and feldspar must play a relatively minor role in the generation of the high Sr phonolitic rocks; a conclusion supported by the rare earth element patterns. None of the phonolitic rocks have Mg numbers or transition metal contents consistent with them being primary melts and since they cannot be related to a single line of descent, the spectrum of phonolitic compositions must derive from a spectrum of basaltic parental magmas. Such a range of basaltic compositions could, as Norry et al. (1980) suggest arise because of the effects of carbonatitic metasomatism in the mantle source region. A mantle peridotite veined by carbonatitic or possibly nephelinitic material could provide a source for basalts, ranging from strongly undersaturated to transitional alkalic. Increasing fCO_2 during melting of peridotite gives rise to increasingly undersaturated melts (Eggler 1974) and since the vein component could be expected to be relatively high in large ion lithophile and high field strength cations as well as volatiles (CO_2, F, Cl, and H_2O) low degrees of melting at high fCO_2 would develop melts relatively enriched in Ti, P, Sr, Rb, Zr, Nb and Ba. Higher degrees of melting would develop less undersaturated basaltic melts, less enriched in these elements. There is now considerable evidence for mantle heterogeneity on a fine scale from regional studies of basaltic provinces (e.g. Norry et al. 1980; Erlank et al. 1980), from studies of inclusions in kimberlites (e.g. Gurney and Harte 1980) and from composite studies (e.g. Menzies and Murthy 1980).

In contrast to the phonolitic suite the trachyte suite, as represented in our sample set, could derive by low pressure (crustal) crystal fractionation from a transitional alkalic basaltic parent. The basalts parental to the trachyte suite were generated from a less metasomatized and consequently slightly less radiogenic source.

Concluding remarks

The phonolitic and trachytic eruptives and intrusives of the summit region of Mt. Kenya represent magmas evolved by crystal fractionation taking place at various levels within the crust or upper mantle. Some members of both the trachytic and phonolitic suites show clear evidence of involvement of feldspar in their genesis; they are strongly depleted in Eu, Ba, Sr and Ca and have developed by crystal fractionation taking place in the crust, from basalts or more evolved magmas. In contrast, some phonolitic rocks are characterized by low SiO_2, relatively high MgO, CaO, TiO_2, P_2O_5, Sr and Ba even though total alkalies, Rb, Zr, Nb and Th are very high. These rocks must be derived from strongly undersaturated, large ion lithophile- and high field strength cation-enriched parents with feldspar playing a much less significant role in their evolution.

A possible source for the spectrum of basaltic parental materials required is a mantle which has undergone recent penetration (metasomatism) by carbonatitic magmas.

Acknowledgements. The authors wish to thank Dr. B.H. Baker and Prof. D.S. Coombs for their extremely useful reviews and Prof. A.J.R. White for stimulating discussion. Mr. I. McCabe assisted with analytical work. We acknowledge the support of NSF grants 78-23423 and 82-18982 and the M.I.T. nuclear reactor. D.J. Jenning's assisted in the field. RWJ publishes with the permission of the Director of the Bureau of Mineral Resources.

References

Bailey DK (1964) Crustal warping – a possible control of alkaline magmatism. J Geophys Res 69:1103–1111

Bailey DK, Schairer JF (1966) The system Na_2O-Al_2O_3 – Fe_2O_3-SiO_2 at 1 atmosphere, and the petrogenesis of alkaline rocks. J Petrol 7:114–170

Baker BH (1967) Geology of the Mount Kenya area. Geol Surv Kenya Rept 79

Baker BH, Williams LAJ, Miller JA, Fitch FJ (1971) Sequence and geochronology of the Kenya rift volcanics. Tectonophysics 11:191–215

Baker BH, Goles GG, Leeman WP, Lindstrom MM (1977) Geochemistry and petrogenesis of a basalt-benmoreite-trachyte suite from the southern part of the Gregory Rift, Kenya. Contrib Mineral Petrol 64:303–332

Bell K, Powell JL (1970) Strontium isotopic studies of alkaline rocks: the alkalic complexes of Eastern Uganda. Bull Geol Soc Am 81:3481–3490

Coombs DS, Wilkinson JFG (1969) Lineages and fractionation trends in unersaturated volcanic rocks from the East Otago volcanic province (New Zealand) and related rocks. J Petrol 10:440–501

Drake MJ, Weill DF (1975) Partition of Sr, Ba, Ca, Y, Eu^{2+}, Eu^{3+} and other REE between plagioclase feldspar and magmatic liquid: an experimental study. Geochim Cosmochim Acta 39:689–712

Eggler DH (1974) Effect of CO_2 on the melting of peridotite. Carnegie Inst Wash Yearb 73:215–224

Erlank AJ, Allsopp HL, Duncan AR, Bristow JW (1980) Mantle heterogeneity beneath Southern Africa: evidence from the volcanic record. Phil Trans R Soc Lond A 297:273–293

Gill RCO (1972) Chemistry of peralkaline phonolite dykes from the Gronnedal-Ika area, South Greenland. Contrib Mineral Petrol 34:87–100

Goles GG (1976) Some constraints on the origin of phonolites from the Gregory Rift, Kenya, and inferences concerning basaltic magmas in the Rift System. Lithos 9:1–8

Green DH, Edgar AD, Beasley P, Kiss E, Ware NG (1974) Upper mantle source for some hawaiites, mugearites and benmoreites. Contrib Mineral Petrol 48:33–43

Gurney JJ, Harte B (1980) Chemical variations in upper mantle nodules from southern African kimberlites. Phil Trans R Soc Lond A 297:273–293

Hamilton DL, Mackenzie WS (1965) Phase-quilibrium studies in the system $NaAlSiO_4$ (nepheline) – $KAlSiO_4$ (kalsilite) – SiO_2-H_2O. Mineral Mag 34:214–231

Irving AJ, Price RC (1981) Geochemistry and evolution of lherzolite-bearing phonolitic lavas from Nigeria, Australia, East Germany, and New Zealand. Geochim Cosmochim Acta 45:1309–1320

Laughlin AW, Brookins DG, Kudo AM, Causey JD (1971) Chemical and strontium isotopic investigations of ultrafamic inclusions and basalt, Bandera Crater, New Mexico. Geochim Cosmochim Acta 35:107–113

Leake BE (1978) Nomenclature of Amphiboles. Mineral Mag 42:533–563

Lippard SJ (1973) The petrology of phonolites from the Kenya Rift. Lithos 6:217–234

Menzies M, Murthy RV (1980) Enriched mantle: Nd and Sr isotopes in diopsides from kimberlite nodules. Nature 283:634–636

Nash WP, Carmichael ISE, Johnson RW (1969) The mineralogy and petrology of Mount Suswa, Kenya. J Petrol 10:409–439

Norrish K, Chappell BW (1967) X-ray fluorescence spectrography. In: Zussman J (ed). Physical methods in determinative Mineralogy. Academic Press, London

Norrish K, Hutton JT (1969) An accurate x-ray spectrographic method for the analysis of a wide range of geological samples. Geochim Cosmochim Acta 33:431–454

Norry MJ, Truckle PH, Lippard SJ, Hawkesworth CJ, Weaver

SD, Marriner GF (1980) Isotopic and trace element evidence from lavas, bearing on mantle heterogeneity beneath Kenya. Phil Trans R Soc Lond A 297:259–271
Price RC, Chappell BW (1975) Fractional crystallization and the petrology of Dunedin Volcano. Contrib Mineral Petrol 53:157–182
Price RC, Compston W (1973) The geochemistry of the Dunedin Volcano: Strontium isotope chemistry. Contrib Mineral Petrol 42:55–61
Price RC, Green DH (1972) Lherzolite nodules in a "mafic phonolite" from north-east Otago, New Zealand. Nat Phys Sci 235:133–134
Ridley WI (1970) The petrology of the Las Canadas Volcanoes, Tenerife, Canary Islands. Contrib Mineral Petrol 26:124–160
Rock NMS (1976) The comparative strontium isotopic composition of alkaline rocks: New data from Southern Portugal and East Africa. Contrib Mineral Petrol 56:205–228
Sceal JSC, Weaver SD (1971) Trace element data bearing on the origin of salic rocks from the Quaternary volcano Paka, Gregory Rift, Kenya. Earth Planet Sci Lett 12:327–331
Weaver SD, Sceal JSC, Gibson IL (1972) Trace element data relevant to the origin of trachytic and pantelleritic lavas in the East African Rift System. Contrib Mineral Petrol 36:181–194
White CM, Taipa MDM, Schilling J (1979) The petrology and geochemistry of the Azores Islands. Contrib Mineral Petrol 69:201–213
Williams LAJ (1971) The volcanics of the Gregory Rift Valley, East Africa. Bull Volcanol 34:439–465
Wooley AR, Symes RF (1967) The analcime-phyric phonolites (blairmorites) and associated analcime kenytes of the Lupata Gorge, Mocambique. Lithos 9:9–15
Wright JB (1966) Olivine nodules in a phonolite of the East Otago alkaline province, New Zealand. Nature 210:519
Wright JB (1969) Olivine nodules and related inclusions in trachyte from the Jos Plateau, Nigeria. Mineral Mag 37:370–374
Wright TL, Doherty PC (1970) A linear programming and least squares computer method for solving petrologic mixing problems. Bull Geol Soc Am 81:1995–2008
Zielinski RA, Frey FA (1970) Gough Island: Evaluation of a fractional crystallization model. Contrib Mineral Petrol 29:242–254

Accepted January 8, 1985